



# Systematic development by the design-of-experiment approach and physicochemical evaluations of the optimized self-microemulsifying astaxanthin delivery system

Mo Mo Ko Zin<sup>1,2</sup>, Veerakiet Boonkanokwong<sup>2</sup>

<sup>1</sup>Graduate Program of Pharmaceutical Sciences and Technology, Faculty of Pharmaceutical Sciences, Chulalongkorn University, Bangkok, Thailand, <sup>2</sup>Department of Pharmaceutics and Industrial Pharmacy, Faculty of Pharmaceutical Sciences, Chulalongkorn University, Bangkok, Thailand

## Corresponding Author:

Veerakiet Boonkanokwong,  
Department of Pharmaceutics  
and Industrial Pharmacy,  
Faculty of Pharmaceutical  
Sciences, Chulalongkorn  
University, Bangkok, Thailand.  
Tel: +66-2218-8275.  
E-mail: veerakiet.b@pharm.  
chula.ac.th

Received: Dec 27, 2020

Accepted: May 2, 2021

Published: Jun 15, 2021

## ABSTRACT

A self-microemulsifying delivery system (SMEDS) containing astaxanthin (AST) was developed and optimized using a mixture design and its desirability function. Independent factors studied in the experimental design were the amounts of castor oil, Cremophor® RH 40, and Tween® 80 in a formula. The measured response variables included droplet size, polydispersity index (PDI), zeta potential, active ingredient content, and transmittance of microemulsions obtained from the AST SMEDS formulations. The desirability function was then adjusted to optimize the formulation. The optimized AST SMEDS was composed of 19.59% castor oil, 62.34% Cremophor® RH 40, and 18.03% Tween® 80, and the resulting self-microemulsions had an average droplet size of 22.55 nm with PDI of 0.27, zeta potential of -9.35 mV, 96.49% of AST content, and 98.80% of transmittance. Our results also showed the optimized formula could rapidly formed (self-emulsification time ~44 s) AST microemulsions with good physicochemical properties and stability conducted by the freeze-thaw study. Moreover, the *in vitro* release profiles of AST from the optimized SMEDS formulation were significantly improved compared to a marketed preparation and raw AST powder. The design of experiments and optimization of these novel AST SMEDS formulations were a promising approach to enhance dissolution of poorly water-soluble AST.

**Keywords:** Astaxanthin, Self-microemulsifying delivery system, Mixture design, Optimization, Antioxidant

## INTRODUCTION

Astaxanthin (AST) is a ketocarotenoid compound naturally found in microorganisms, such as freshwater microalgae *Haematococcus pluvialis* and yeast *Xanthophyllomyces dendrorhous*,<sup>[1]</sup> and remarkably known for its extremely powerful antioxidant activity. The antioxidant activity of AST is 10 times more effective than that of other carotenoids<sup>[2]</sup> and over 500 times higher than that of vitamin E.<sup>[3]</sup> Due to its powerful antioxidant activity, extensive applications of AST have been observed in livestock feeds, foods, nutraceuticals, cosmetics, and pharmaceuticals. Research in recent years has indicated that AST possesses an inhibitory effect on inflammation and oxidative stress.<sup>[4]</sup> In addition, due to AST's chemical structure, this substance

can easily cross the blood-brain barrier and has a powerful protective effect on human brain.<sup>[5]</sup> Nowadays, AST has gained much interest for its effect on the prevention or co-treatment of neurodegenerative diseases such as Parkinson's and Alzheimer's diseases.<sup>[6]</sup>

However, due to the highly unsaturated structure of an AST molecule, it is very sensitive to light, oxygen, and temperature, and thus prone to oxidation, isomerization, and degradation.<sup>[7]</sup> Moreover, the bioavailability of AST is greatly reduced due to its terribly poor solubility in water, resulting in negative effects on its practical applications.<sup>[8]</sup> For those aforementioned reasons, it is necessary to systematically develop methods to broaden the range of AST applications to successfully delivery this active substance to the target cells

at an effectively therapeutic level. Different approaches, such as micro/nanoencapsulation<sup>[6]</sup> and formulation of liposomes<sup>[8]</sup> and nanoparticles,<sup>[9]</sup> have been investigated to enhance the aqueous solubility, bioavailability, and stability of AST. Nonetheless, complex methods of formations and high costs of ingredients involved are required in these formulations.

A self-microemulsifying delivery system (SMEDS), an advantageous method for the delivery of poorly aqueous-soluble compounds, is a simple formulation produced by a simple technique as well as required less time of formulation and available cheap excipients.<sup>[10]</sup> Its ability to form fine oil-in-water (o/w) micro/nanoemulsions under gentle stirring after diluting with water is the basic principle of this system.<sup>[11]</sup> The active ingredient is generally shown in a solubilized form in the SMEDS, resulting in spontaneous micro/nanoemulsion formation in the gastrointestinal (GI) tract. The small size of the formed micro/nanoemulsion droplets provides a large interfacial surface area for the compound absorption through small intestinal epithelial cells.<sup>[12]</sup> A number of formulation-related parameters, including surfactant concentration, oil/surfactant ratio, polarity of emulsions, droplet size and charge, are needed to be carefully considered as they have a tremendous impact on the efficiency of oral absorption of a biologically active compound incorporated in the SMEDS, and the self-emulsification ability is also determined by those parameters.<sup>[13,14]</sup> Only appropriate combination of exclusively specific pharmaceutical excipients can lead to efficient self-emulsifying systems.

Over the past few years, a design of experiment (DoE) approach, which is one of the important building blocks for the quality by design framework, has become increasingly prevalent in optimization of formulations to better understand how material attributes and process parameters affect characteristics of the formulations. DoE can be employed to find the optimum proportion of the SMEDS excipients and to improve the product quality attributes and ultimately the product quality target profile.<sup>[15-17]</sup> DoE methodology allows for precise estimation of the effects of the input factors and the interactions of each variable with proportionally fewer numbers of experimental runs enabling the optimization process more efficient. A mixture design, one of the experimental designs commonly employed in the DoE approach, is utilized when the overall amount of a composition is determined and the excipient ratio in a formulation is rationalized. Optimization of oil/surfactant/co-surfactant ratios in a SMEDS formula is one of the common applications of mixture design in pharmaceutical technology. For instances, Bhattacharya *et al.*<sup>[18]</sup> successfully formulated and optimized the docetaxel-loaded self-microemulsifying drug delivery system using the mixture design. In another research, Sandhu *et al.*<sup>[19]</sup> well designed a tamoxifen-loaded self-nanoemulsifying formulations by a mixture design. The optimized formulation showed an increased cellular uptake and enhanced bioavailability of tamoxifen. Optimizing the settings and finding the compromising conditions for all input variables could be considered for more than one favorable output responses.<sup>[20]</sup> More details on the DoEs related to multiple responses optimization were given in articles by Singh *et al.*<sup>[21]</sup> and Li *et al.*<sup>[22]</sup>

This present work attempted to develop the SMEDS formulation for solving the solubility, bioavailability, and stability problems of poorly aqueous-soluble AST using the concept of the mixture design. The objective of this research was to investigate the effects of formulation-related variables, that is, the amounts of the oil phase, surfactant, and cosurfactant, and their interactions on various physicochemical characteristics of the AST SMEDS formulations. In this study, the mixture design was employed for the experimental plan, and the effects of the varying components in the formula on the properties of AST-loaded SMEDS were graphically interpreted using three-dimensional (3D) plots. Optimization of the quantities of input materials in the AST SMEDS was then successfully achieved through a predictive mathematical modeling. The developed SMEDS containing AST formulations were evaluated on various parameters using different techniques, such as physical appearance by visual observation, measurement of emulsification time, refractive index, emulsion droplet size and image by transmission electron microscopy (TEM), and freeze-thaw stabilities. Furthermore, *in vitro* release studies of AST in the optimized SMEDS formulation were performed, and the dissolution profiles were compared with those of AST marketed preparation and raw material powder. We ultimately hope that this novel AST self-microemulsifying platform can be a future candidate for delivering the biologically active substance to target cells in the body and that this AST product will be able to help mitigating symptoms in elderly patients undergoing with neurodegenerative diseases.

## MATERIALS AND METHODS

### Materials

AST (CAS Number: 472-61-7), purified grade containing  $C_{40}H_{52}O_4$  at least 98.09%, was purchased from Hangzhou Dayang Chem Co., Ltd. (Hangzhou, China). Castor oil, polyoxyl 40 hydrogenated castor oil (Cremophor® RH 40), and polysorbate 80 (Tween® 80) were purchased from Srichand United Dispensary, Co., Ltd. (Bangkok, Thailand). All other chemicals and reagents used in this research work were of analytical grade purity. One commercially available product in the dosage form of soft gelatin capsule containing AST 4 mg was purchased for comparison of dissolution and release profiles with our SMEDS formulations.

### Methods

#### *Pseudoternary phase diagram construction*

Based on the hydrophilic-lipophilic balance (HLB) and our preliminary results,<sup>[23]</sup> castor oil, Cremophor® RH 40 (HLB value of 14–16), and Tween® 80 (HLB value of 15) were selected as components in the SMEDS because of high solubility of AST in these substances. Self-microemulsifying systems were prepared by varying concentrations of castor oil as an oil phase, Cremophor® RH 40 as a surfactant, and Tween® 80 as a cosurfactant. Castor oil can be classified as a long-chain triglyceride (LCT) with each of its three hydroxyl groups esterified with a long-chain fatty acid, principally ricinoleic acid. At the ambient temperature, pseudoternary phase diagrams were created by using the water titration method to examine the concentration of constituents for the predominant range of microemulsion formation.<sup>[24]</sup>

The chosen surfactant (Cremophor® RH 40) and cosurfactant (Tween® 80) were combined at five fixed proportions (1:1, 2:1, 3:1, 4:1, and 5:1 by weight) to set up various surfactant/cosurfactant mixtures ( $S_{mix}$ ). It was then followed by the addition of castor oil to the individual  $S_{mix}$  at different oil:  $S_{mix}$  ratios (9:1, 8:2, 7:3, 6:4, 5:5, 4:6, 3:7, 2:8, and 1:9 by weight). After the incorporation of water (5% stepwise increments) to each mixture, gentle swirling of the mixture was performed. For transparency and turbidity, visual observation of the mixture was started and recorded after every drop-wise addition of water. At this stage, the proportions of oil with surfactant/cosurfactant ( $S_{mix}$ ) and water were calculated in percentage. Pseudoternary phase diagrams were constructed according to these percentages, and the microemulsion forming regions were identified using the Chemix School™ software.

#### Optimization of AST-loaded SMEDS formulations using a mixture design

Minitab™ software (version 17.0; Minitab™ Inc., State College, PA, USA) was used for developing and evaluating the experimental design. The mixture design was deployed to optimize the compositions in the AST SMEDS formulations. The experiments were designed using three components as independent variables. Based on the solubility study and the pseudoternary phase diagram, concentrations of castor oil (oil phase;  $X_1$ ), Cremophor® RH 40 (surfactant;  $X_2$ ), and Tween® 80 (cosurfactant;  $X_3$ ) were set within ranges of 10–40%, 48–72%, and 12–18%, respectively. For any experiment, the concentrations of AST,  $X_1$ ,  $X_2$ , and  $X_3$  added up to 100% in a mixture design. Droplet size ( $Y_1$ ; nm), polydispersity index (PDI) ( $Y_2$ ), zeta potential ( $Y_3$ ; mV), active ingredient content ( $Y_4$ ; %), and transmittance ( $Y_5$ ; %) were examined as the response variables to optimize the formulation with excellent physiochemical characteristics. The basic mixture design allowed 13 experiments to fit a model, estimate experimental errors in the responses, and check for lack of fit of the model. After the influences of input variables ( $X_n$ ) on the responses ( $Y_n$ ) were studied, accuracy and reliability of the estimation using the desirability functions were evaluated by calculating prediction errors (%) which were computed by the following equation:

$$\text{Prediction error (\%)} = \frac{\text{Measured value} - \text{Predicted value}}{\text{Measured value}} \times 100(\%) \quad (1)$$

#### Preparation of AST-loaded SMEDS

Thirteen formulations were designed and developed from the design space generated in the Minitab™ software. The determination on the quantity to be taken for excipients relied on the microemulsification area in the pseudoternary phase diagram. AST was precisely weighed and dissolved in castor oil. The oily mixture was then warmed at 37°C using a water bath. The mixture was later combined with surfactant and cosurfactant at a specified ratio and then agitated with a magnetic stirrer for 10 min. Furthermore, sonication of the AST SMEDS formulations was performed at 40°C for 15 min.<sup>[24]</sup> To avoid adverse effects from light and oxygen and to prevent degradation of AST, all AST SMEDS formulations were prepared in a cool place under minimal exposure to light and kept in tight amber containers, and where possible, covered with aluminum foils during production and all further testing processes.

#### Droplet size and PDI measurement

One of the important characteristics of micro/nanoemulsions can be determined by the measurement of emulsion droplet size which will affect the rate and extent of drug release as well as absorption. The information about droplet size distribution can be provided by the examination of PDI. The uniform and narrow particle size distribution is suggested by the low value of PDI. To commence PDI measurement, approximately 0.1 ml of each SMEDS formulation and 25 ml of distilled water (dilution in 1:250 ratio) was constantly stirred in a glass beaker.<sup>[18]</sup> The resulting emulsion was then subjected to particle size analysis. The droplet size and droplet size distribution (PDI) of the resultant microemulsions were determined by a dynamic light scattering analyzer (Malvern Zetasizer™, UK). The preparation was transferred to a cuvette and measured with a fixed angle of 90°. After equilibrium, the particle (droplet) size and PDI were recorded. All studies were repeated in triplicate.

#### Zeta potential measurement

The zeta potential value indicates the physical stability of diluted emulsions. It is the measurement of electric charges at the surface of particles. The values were examined by determining electrophoretic mobility of the particles. In this research project, zeta potential was determined using Zetasizer™ (Malvern Zetasizer™, UK). The suitable dilution of the SMEDS sample was performed with distilled water (1:250), and the diluted preparation was placed in a disposable zeta cell.<sup>[18]</sup> All samples were measured in triplicate. The zeta potential value results were reported as mean  $\pm$  standard deviation (SD).

#### Active ingredient (AST) content measurement

According to the previous research,<sup>[25]</sup> it was reported that a combination of solvents was more advantageous to enhance solubility of carotenoids than a single solvent. In our study, a solvent mixture was used to extract AST in the self-microemulsion samples. The samples were appropriately diluted with an organic solvent mixture (dichloromethane [DCM]: methanol [MeOH] = 1:4 v/v). The preparation of samples was performed in triplicate, and the absorbance was measured after suitably diluting the samples. An ultraviolet (UV)-visible spectrophotometer was utilized in the quantification of AST amount at the 480-nm wavelength.<sup>[26]</sup> The solvent mixture of DCM and MeOH at the same ratio was used as a blank. From a calibration plot, calculation of the AST content in each SMEDS formulation was performed. More details can be found in the Appendix.

#### Percent transmittance measurement

When the clear and transparent microemulsion formation is obtained, the value of transmittance is close to 100%.<sup>[27]</sup> Transparency of a SMEDS formulation was examined spectrophotometrically at the wavelength of 650 nm after appropriate dilution of formulation with distilled water (1:250). Deionized water was kept as blank. All samples were measured in triplicate.

#### Visual observation of self-microemulsions

For the physical appearance of the AST-contained microemulsions obtained from SMEDS, visual determination of

the optimized formulations was completed. The formulations were subjected to dilute with distilled water (1:250), and the diluted microemulsions were followed by stirring for 1 min and stored up to 24 h. After that, any signs of phase separation and/or precipitation of AST were visually detected.<sup>[28]</sup> The visual grading system of the SMEDS could be classified as follows: (a) denoting a rapidly forming (within 1 min) microemulsion that was clear or slightly bluish in appearance, (b) denoting a rapidly forming, slightly less clear emulsion that had a bluish white appearance, (c) denoting a bright white emulsion (similar in appearance to milk) that formed within 2 min, (d) denoting a dull, grayish white emulsion with a slightly oily appearance that was slow to emulsify (longer than 2 min), and (e) denoting a formulation that exhibited either poor or minimal emulsification with large oil droplets present on the surface.

#### *Self-emulsification time*

To examine the effectiveness of self-microemulsification, each optimized formulation was subjected to dilute with distilled water (1:250) and stirred constantly at 100 revolutions per minute (rpm) and at  $37 \pm 0.5^\circ\text{C}$ .<sup>[29]</sup> Subsequently, the time period needed to form microemulsion was recorded, and the test was performed in triplicate.

#### *Refractive index measurement*

The value of refractive index demonstrates that the formulation is transparent in nature. If a refractive index value of self-microemulsions obtained from the SMEDS formulation is similar to that of water (1.333), then the formulation has transparency. This measurement was done by using a refractometer (Mettler Toledo™, Thailand). The dilution of the optimized formulations was performed with distilled water (1:250), and one drop of the diluted formulation was placed on the slide. The refractive index value of the diluted formulation was then measured and compared to that of water.<sup>[30]</sup> The sample was measured in triplicate.

#### *TEM*

Self-microemulsions obtained from the optimized SMEDS formulation were determined for morphological analysis using TEM (TEM; JEOL USA JSM-6700F) as an imaging aid. The formulations were diluted, and a single drop of the diluted sample was placed on the holey film grid and stained with a 2% aqueous solution of phosphotungstic acid and allowed to dry before being observed under the electron microscope.<sup>[30]</sup> The digital microscopic camera was used to record the TEM micrographs.

#### *Freeze-thaw stability studies*

Dilution of the optimized AST SMEDS formulation was performed with distilled water (1:250) to obtain microemulsions immediately before the stability testing. Droplet size, PDI, zeta potential, and the active ingredient content of the self-assembling microemulsions were examined for instability issues.<sup>[31,32]</sup> The freeze-thaw test was performed for three cycles at temperatures of  $-20^\circ\text{C}$  and  $25^\circ\text{C}$ . At each temperature in a cycle, the self-microemulsion samples were stored at least 48 h, and those physicochemical stability results were carried out. All tests were done in triplicate.

#### *In vitro release studies*

With the use of a dialysis bag diffusion technique adapted from a research work of Deshmukh and Kulkarni,<sup>[33]</sup> the *in vitro* release study of AST from the optimized SMEDS formulation was conducted and compared to raw material AST powder and one marketed preparation of the same dose per unit. A commercial soft gelatin capsule product contained 4 mg (typical labeled amount) of AST which was solubilized and suspended in an oleic safflower oil, d-alpha-tocopherol, and glycerin. AST powders as received from the supplier were also employed in the dissolution evaluation. For better understanding the dissolution behavior of AST in the GI tract, the release of AST from the optimized SMEDS formulation was further studied by changing pH sequentially.<sup>[34]</sup> The dissolution media used in these tests were HCl/NaCl buffer pH 1.2 for the first 30 min, acetate buffer pH 4.5 for the next 1.5 h, and phosphate buffer pH 7.4 for the past 6 h to simulate varying pH conditions along and the time period during which the dosage form spent in the digestive system. Before performing the experiments, dialysis bags (Fisherbrand™ Regenerated Cellulose Dialysis Membrane, molecular weight cut-off 12,000 Da) were hydrated overnight. One gram of the optimized SMEDS formulation (containing 4 mg of AST) was positioned in a dialysis bag. The dialysis bags were immersed in 900 ml of medium rotated at 100 rpm and maintained in a  $37^\circ\text{C}$  dissolution bath (covered with aluminum foils). 10 ml of samples were collected at predetermined time intervals of 5 min, 10 min, 15 min, 30 min, 1 h, 2 h, 4 h, and 8 h. It was then refilled with similar volume of the tested medium to compensate for the loss due to sampling and maintain the sink condition.<sup>[24,35]</sup> An UV-visible spectrophotometer was used for the analysis of the AST content in the aliquots at the wavelength of 480 nm according to the method described in the earlier section. All samples were measured in triplicate.

### **Statistical Analysis**

All data are expressed as mean  $\pm$  SD. Statistical significance was determined using the Student's *t*-test with  $P < 0.05$  considered to be statistically significant. Minitab™ software was used to determine statistical values of all the responses.

## **RESULTS AND DISCUSSION**

### **Optimization of SMEDS Compositions**

Optimization of the SMEDS compositions will be performed in two sequential steps. Firstly, the amounts of components will be varied to identify regions where self-microemulsions will be spontaneously formed and construct pseudoternary phase diagrams. Preliminary ranges of the amount of each ingredient used in the SMEDS formulations will be acquired. Subsequently, the lower and upper limits of the compositions will be specified in the experimental program to generate SMEDS formulations in a mixture design.

#### *Pseudoternary Phase Diagrams of SMEDS*

There are different volumes of the gastric liquid in the stomach at various time points during the day. The AST SMEDS should form emulsions with the droplet size preferably within the nano to micro scales and without precipitation of the active

substance when the formulation is diluted with gastric fluid in the stomach or with distilled water in an experiment test tube. It was observed that the emulsification capacity is tremendously related to the amounts of oil, surfactant, and cosurfactant in formulations as well as the volume of water phase in the medium.<sup>[36]</sup> In this work, pseudoternary phase diagram was developed for determining the self-microemulsifying area and for calculating the concentrations of oil, surfactant, and cosurfactant in the SMEDS formula which would lead to stable micro/nanoemulsions. To create the phase diagram, castor oil, Cremophor® RH 40, and Tween® 80 were defined in this research as oil phase, surfactant, and cosurfactant, respectively, according to the solubility data and emulsification studies. Our preliminary data showed that the solubilities of AST in castor oil, Cremophor® RH 40, and Tween® 80 were equal to 155.87, 252.75, and 256.71 µg/ml, respectively.<sup>[23]</sup> When titrated with deionized water under mild agitation, SMEDS formed micro- and nanoemulsions with the droplet size <200 nm. This is a thermodynamically spontaneous emulsification process as the energy needed for the formation of micro/nanoemulsions is very low.<sup>[37]</sup> A surfactant has a role to facilitate this self-emulsification process. In the presence of a surfactant, a layer is formed around the oil globule in such a way that the polar heads of the surfactant pull out the water phase and the nonpolar tails lie toward lipid phase, resulting in a decrease in the surface energy between the oil-water interface.<sup>[38]</sup> Moreover, the mixture of surfactant and cosurfactant ( $S_{mix}$ ) ratio is another important factor having an effect on the microemulsion formation and stability as a mechanical barrier to droplet coalescence is provided by adsorbing the surfactant/cosurfactant at the interface.<sup>[39]</sup> A cosurfactant with an appropriate concentration range is also crucial to the formation of micro/nanoemulsions. Due to the high-water solubility of the cosurfactant chosen in this study, becoming less stable microemulsion systems will be caused by an excess amount of the cosurfactant. This may lead to an increase in the droplet size due to the expanding interfacial films.<sup>[10]</sup>

To begin our research, pseudoternary phase diagrams of the Cremophor® RH 40:Tween® 80 mixtures ( $S_{mix}$ ) at five various ratios (i.e., 1:1, 2:1, 3:1, 4:1, and 5:1 by weight) were developed for castor oil using a water-titration method. Preparation of the surfactant plus cosurfactant mixtures was followed by the addition of castor oil to the individual  $S_{mix}$  at different oil:  $S_{mix}$  ratios (i.e., 9:1, 8:2, 7:3, 6:4, 5:5, 4:6, 3:7, 2:8, and 1:9 by weight). The visual observation was then performed and recorded after pipetting down 5% increment of water to each of the mixture of oil and  $S_{mix}$ . At the same time, the proportions of castor oil and  $S_{mix}$  were also calculated. Using the Chemix School™ software, a separate diagram was developed for each  $S_{mix}$  ratio, and the visual observation was also recorded for each diagram. Based on the visual observation, only the combinations in SMEDS formulations of which clear and transparent microemulsions noticed were plotted on the self-microemulsifying regions in the diagrams. In the pseudoternary phase diagram, the black region represented the self-microemulsification area.

Pseudoternary phase diagrams for the SMEDS formulations containing castor oil, Cremophor® RH 40 as a surfactant, and Tween® 80 as a cosurfactant at different  $S_{mix}$  ratios (1:1 to 5:1) are presented in Figure 1a-e, respectively. A comparatively largest

microemulsion region was obtained for the  $S_{mix}$  proportion of Cremophor® RH 40:Tween® 80 = 4:1, as can be seen in Figure 1d, compared to the other ratios in the SMEDS formulations. At this combination, the designed SMEDS may possess the optimal required HLB value (which was approximately 14) to produce stable castor oil-based microemulsions. It was also showed that an increase in the Cremophor® RH 40 amount in the surfactant mixture (i.e., increasing the  $S_{mix}$  ratio) led to the expansion of the microemulsion formation area in the pseudoternary phase diagram except for the 5:1 ratio. Another observation was that poor microemulsion was formed with high concentration of oil in all cases. This may be due to very less amount of water in and low entrapment capacity of the formed microemulsions upon dilution.<sup>[40]</sup>

Furthermore, the effect of adding AST 0.04% w/w of the SMEDS formulation into the selected formula composed of Cremophor® RH 40:Tween® 80 = 4:1 was also evaluated. Dissolving AST in castor oil was performed until a clear dark purple to brown oily solution was achieved, which was then followed by mixing with the surfactant/cosurfactant mixture. The boundary of the microemulsion region in the pseudoternary phase diagram was examined by repetition of the water-titration procedure in the presence of the active substance AST. It was observed in Figure 1d and f that the boundaries of the self-microemulsification area did not change, thus the addition of AST into the blank SMEDS formulation containing Cremophor® RH 40:Tween® 80 in the 4:1 ratio had no significant impact on the microemulsion regions and the self-microemulsifying ability of the SMEDS formulation.

As can be noticed from the pseudoternary phase diagrams, reasonably large total amounts of surfactant and cosurfactant were combined in the SMEDS formulations to form spontaneous self-microemulsions after an oral administration. One might ask whether the SMEDS formulations containing large amounts of surfactants are safe and appropriate for an oral delivery. Nonionic surfactants, such as the ones that we used in this work, were often considered in formulating SMEDS because of their good physicochemical stability, being less affected by pH and ionic strength changes, high degree of compatibility with other components in a formula, and relatively low toxicity.<sup>[41,42]</sup> Rachmawati *et al.*<sup>[43]</sup> evaluated the safety of using a large amount of polyoxyl 40 hydrogenated castor oil as a surfactant in oral nanoemulsion formulations. This study showed that emulsions containing high percentage of Cremophor® RH 40 in a formula caused insignificant GI irritation and other adverse events, and they concluded that Cremophor® RH 40 used in a large amount was rationally suitable for an oral delivery system. However, we might need to confirm the safety of our AST SMEDS formulations by performing *in vitro* and/or *in vivo* tests in the future research.

#### Mixture design of AST SMEDS and statistical analysis

We set up a mixture design in the program and studied the effect of the ratio of the formulation excipients on the responses (dependent variables). It has been reported in previous research.<sup>[44,45]</sup> that the primary factors affecting the *in vitro* dispersion of the SMEDS preparations were considered to be the quantity of the oil phase, surfactant, and cosurfactant.

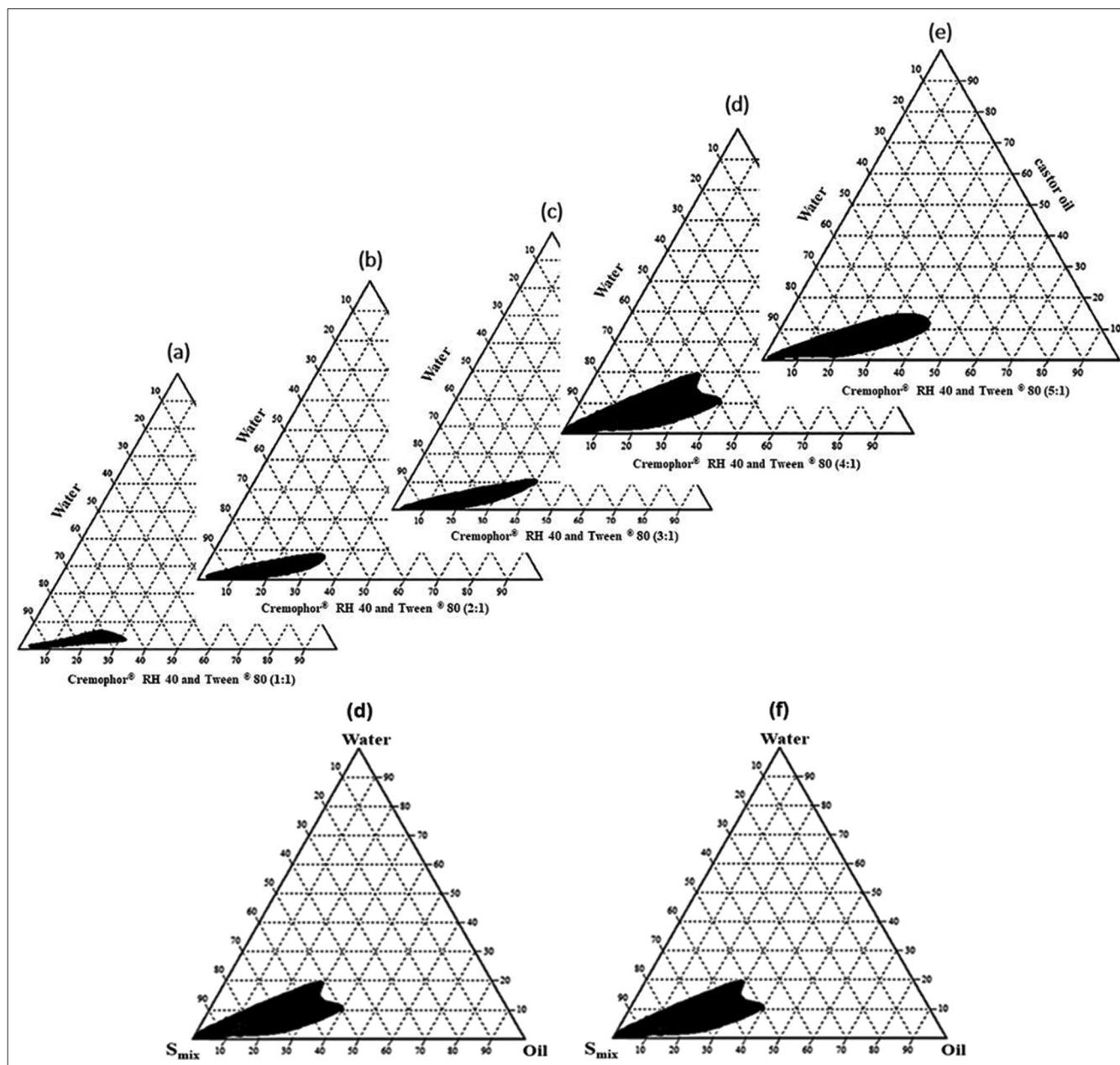


**Figure 1:** (Top) Pseudoternary phase diagrams for the blank self-microemulsifying delivery system (SMEDS) formulations composed of castor oil, Cremophor® RH 40, and Tween® 80 for the surfactant/cosurfactant  $S_{mix}$  (Cremophor® RH 40:Tween® 80) mixture ratios of (a) 1:1, (b) 2:1, (c) 3:1, (d) 4:1, and (e) 5:1. (Bottom) A comparison between pseudoternary phase diagrams constructed for (d) blank SMEDS formulation and (f) Astaxanthin-incorporated SMEDS formulation at the selected  $S_{mix}$  ratio=4:1

Limits of each composition in SMEDS formulations were set based on the results of the self-emulsification regions (oil +  $S_{mix}$  + water) from the pseudoternary phase diagrams. However, when we employed the optimal mixture design, we set up the levels of the input factors  $X_1$ ,  $X_2$ , and  $X_3$  excluding water in the computer software as shown in Table 1 to ensure that the ranges of independent variables covered the entire experimental design space of our work and to generate reliable and accurate optimization models for each response. After studying the influences of the input variables on the responses, optimization and validation of the AST SMEDS formulation will be next carried out.

**Table 1:** Ranges of independent variables in the mixture design for SMEDS formulations

Independent variables (function)		Range (%w/w)	
		Minimum	Maximum
$X_1$	Castor oil (lipid phase)	10	40
$X_2$	Cremophor® RH 40 (surfactant)	48	72
$X_3$	Tween® 80 (cosurfactant)	12	18

SMEDS: Self-microemulsifying delivery system

As shown in Table 2, details of the three compositions in thirteen formulas (LCT-SMEDS<sub>1-13</sub>) designed and generated

**Table 2:** Values of the three components as independent variables in the AST-loaded LCT-SMEDS formulations and their associated dependent variables (response data) measured ( $n=3$ ) for 13 experiments in the mixture design. The amount of AST is fixed at 0.04% w/w in each formula

Formulation	Independent variables			Dependent variables (Responses)				
	Castor oil ( $X_1$ ; %)	Cremophor® RH 40 ( $X_2$ ; %)	Tween® 80 ( $X_3$ ; %)	Droplet size ( $Y_1$ ; nm)	PDI ( $Y_2$ )	Zeta potential ( $Y_3$ ; mV)	Active ingredient (AST) content ( $Y_4$ ; %)	Transmittance ( $Y_5$ ; %)
LCT-SMEDS <sub>1</sub>	33.9864	47.9808	17.9928	99.93±1.88	0.36±0.07	-11.51±2.96	86.97±0.58	81.67±4.03
LCT-SMEDS <sub>2</sub>	15.9936	71.9712	11.9952	24.36±0.18	0.29±0.10	-10.41±3.47	97.47±2.27	98.35±0.08
LCT-SMEDS <sub>3</sub>	9.9960	71.9712	17.9928	20.17±0.37	0.22±0.01	-9.45±0.77	99.71±0.37	98.57±0.15
LCT-SMEDS <sub>4</sub>	39.9840	47.9808	11.9952	128.74±4.82	0.28±0.01	-11.43±1.62	84.55±0.49	75.72±1.04
LCT-SMEDS <sub>5</sub>	36.9852	47.9808	14.9940	122.09±3.31	0.32±0.08	-11.17±1.42	85.27±0.92	78.48±0.57
LCT-SMEDS <sub>6</sub>	27.9888	59.9760	11.9952	35.00±1.64	0.23±0.04	-12.90±1.48	92.23±0.88	97.41±0.50
LCT-SMEDS <sub>7</sub>	12.9948	71.9712	14.9940	22.91±0.12	0.34±0.01	-12.33±2.03	98.14±0.98	98.50±0.36
LCT-SMEDS <sub>8</sub>	21.9912	59.9760	17.9928	27.70±0.47	0.20±0.07	-11.30±1.91	94.48±0.72	98.11±0.12
LCT-SMEDS <sub>9</sub>	24.9900	59.9760	14.9940	25.57±4.95	0.37±0.03	-11.17±0.98	93.45±1.98	98.07±0.19
LCT-SMEDS <sub>10</sub>	29.4882	53.9784	16.4934	65.21±3.20	0.34±0.05	-9.19±3.13	90.09±1.16	94.88±1.39
LCT-SMEDS <sub>11</sub>	20.4918	65.9736	13.4946	26.96±0.61	0.31±0.02	-9.06±0.94	95.58±1.71	98.15±0.40
LCT-SMEDS <sub>12</sub>	17.4930	65.9736	16.4934	26.07±0.96	0.33±0.01	-8.34±2.14	96.17±0.82	98.31±0.53
LCT-SMEDS <sub>13</sub>	32.4870	53.9784	13.4946	76.04±2.12	0.30±0.02	-8.51±1.17	87.73±1.16	92.28±2.16

LCT-SMEDS: Long-chain triglyceride-self-microemulsifying delivery system

from Minitab™ were specified along with their five responses. Note that the amount of AST was fixed at 0.04% w/w in each formulation. For the thirteen experimental formulas, the droplet size ( $Y_1$ ) of the formed AST-loaded emulsions ranged from 20.17 nm to 128.74 nm with PDI ( $Y_2$ ) ranging from 0.20 to 0.37, which indicated that the nanoemulsion droplets were of generally uniform size. Zeta potential ( $Y_3$ ) ranged from -8.34 mV to -12.90 mV while the active ingredient AST content ( $Y_4$ ) could be assayed between 84.55% and 99.71%, and the transmittance values ( $Y_5$ ) of the slightly transparent to clear nanoemulsions formed could be measured from 75.72% to 98.57%. It was observed that a high amount of castor oil in a formulation (for examples as in LCT-SMEDS<sub>4</sub> and LCT-SMEDS<sub>3</sub>) typically contributed to self-microemulsions with large droplets but less clear physical appearance and less amount of AST entrapped within the system. In such cases, this may be because those formulations consisted of inappropriate amount of surfactant/cosurfactant in the SMEDS.

All response data were next fitted to various mathematical models using the Minitab™ software. All measured dependent variables ( $Y_n$ ) of the AST LCT-SMEDS were stated to be fitted by the linear, quadratic, full cubic and full quartic equation models, and several statistical parameters related to the equation models were reported and compared in Table 3. The sequential  $P$ -values for all responses were <0.0001. A sequential  $P < 0.05$  indicated that the model terms were significant. Multiple regression analyses of the responses for the models were expressed in  $R^2$ , adjusted  $R^2$ , and adequate precision. The percentage of response variable variation ( $R^2$ ) values denoted the total variation explained by the model. The adjusted  $R^2$  values based on their relationships with one or more predictor variables reflected the influence of the increasing or decreasing numbers of model terms. As presented in Table 3, the  $R^2$  values and adjusted  $R^2$  values for all responses were essentially >90%. Similar values of  $R^2$  and adjusted  $R^2$  were desirable for a good model fit. More details for the impacts of the formulation-related material attributes on the quality attributes of the AST LCT-SMEDS will be elaborated in the next sections.

#### Influence on droplet size ( $Y_1$ )

The quality and delivery performance of self-microemulsion systems containing a biologically active substance were primarily determined by the established emulsion droplet size.<sup>[46]</sup> The smaller the microemulsion droplets are, the larger the interfacial surface area they have, and hence, the rapid absorption is promoted as well as the bioavailability of the active compound is improved. Several researchers working on microemulsions and SMEDS recommended that the ideal diameter of stable microemulsions should be 20–200 nm.<sup>[41,47]</sup> In this research, the droplet size of SMEDS after dilution was selected as one of the responses important for *in vitro* evaluation. In the preparation of SMEDS, the smaller the droplet size of SMEDS, the better the result of active ingredient release with higher bioavailability. Therefore, the droplet size ( $Y_1$ ) of the SMEDS formulations was aimed to be minimized and subsequently optimized when considering other factors. Referring to Table 2, the lowest (20.17 ± 0.37 nm) and the highest (128.74 ± 4.82 nm) values of droplet size, respectively, resulted from the formulation LCT-SMEDS<sub>3</sub> and LCT-SMEDS<sub>4</sub>. The suggested quadratic model [Table 3] for

the microemulsion droplet size statistically fitted well to the data. According to the analysis of variance results in Table 4, the program produced the following polynomial equation as expressed in Eq. (2).

$$\text{Droplet size } (Y_1) = 1022 X_1 - 87 X_2 - 7902 X_3 - 2182 X_1 X_2 + 10818 X_1 X_3 + 10539 X_2 X_3 \quad (2)$$

The absolute values of the main factor coefficients, which expressed the importance of the effects of the independent variables, were in the order of  $X_3 \gg X_1 \gg X_2$ . An increase in the amount of castor oil in a formulation may direct toward the enlargement of the developed microemulsion droplets. Moreover, reduction in the mean droplet size may be resulted from the addition of either Cremophor® RH 40 or Tween® 80 into a formula. A large amount of surfactant or cosurfactant could more significantly reduce interfacial tensions between particles and thus make the o/w microemulsion droplets smaller. Accordingly, it can be summarized that the increase in the amount of oil and the decrease in the amount of surfactant/cosurfactant mixture led to the enlargement of SMEDS droplets. It can be also concluded from the  $P < 0.05$  [Table 4] that the average droplet size was significantly influenced by all of the individual factors and the interaction terms (positively and synergistically impacted by  $X_1 X_3$  and  $X_2 X_3$ , but antagonistically affected by  $X_1 X_2$  indicated by the negative value of the coefficient). The relationship between the input variables and the droplet size ( $Y_1$ ) for AST LCT-SMEDS was shown in Figure 2 (3D response surface plots) and Figure 3 (contour plots).

#### Influence on PDI ( $Y_2$ )

The PDI was selected as another critical response since the PDI test results would provide details about the distribution and homogeneity of the emulsion particle size. Particulate matters ordinarily had PDI values between 0.05 and 0.7.<sup>[48,49]</sup> At one extreme, highly uniform microemulsions and very narrow droplet size distribution had been implied by PDI values <0.05. On the contrary, at the other extreme, PDI values larger than 0.7 indicated that the microemulsions had a very broad particle size distribution. Table 2 showed the outcomes of the PDI measurements for all thirteen AST LCT-SMEDS formulas. The PDI values of the LCT-SMEDS formulations were between 0.20 and 0.37. After dilution with water, all the polydispersity values of AST SMEDS were below 0.4, suggesting fairly good uniformity in the microemulsion droplet size distribution. As mentioned in Table 3, the following linear model equation (Eq. (3)) was developed for the PDI of AST LCT-SMEDS.

$$\text{PDI } (Y_2) = 0.2844 X_1 + 0.3416 X_2 + 0.3944 X_3 \quad (3)$$

The importance of the three excipients on PDI was in the order of  $X_3 > X_2 > X_1$  and was at a similar order of magnitude. The positive coefficient values of all input variables in Eq. (3) indicated that an increase in the amount of oil, surfactant, or cosurfactant would raise the PDI of the AST LCT-SMEDS and broaden the microemulsion droplet size distribution. This was probably due to the fact that, when the amount of the ingredient in a formula was changed, not only the required HLB value of the emulsion system was varied from the balance but the droplet size of microemulsions was also altered. For example, if the quantity of Tween® 80 ( $X_3$ ) in the formulation

**Table 3:** Summary of the results of statistical analysis and model equations for the measured responses of the AST LCT-SMEDS formulations

Models	SE	PRESS	R <sup>2</sup> (%)	R <sup>2</sup> (adj) (%)	Remark
Droplet size					
Linear	17.6952	1311.24	80.39	79.31	
Quadratic	10.0087	4312.41	93.90	92.98	Suggested
Full cubic	10.7533	4335.33	93.17	92.36	
Full quartic	10.0203	5873.82	93.46	93.30	
PDI					
Linear	0.0460777	0.0907071	92.02	90.63	Suggested
Quadratic	0.0471451	0.1007071	91.11	90.46	
Full cubic	0.0482528	0.127091	91.03	90.25	
Full quartic	0.0508643	0.15135	82.17	81.72	
Zeta potential					
Linear	2.37366	302.915	82.44	81.02	
Quadratic	2.02908	212.683	98.15	95.22	Suggested
Full cubic	2.24052	240.854	91.79	91.03	
Full quartic	2.28664	246.138	92.21	88.54	
Active ingredient (AST) content					
Linear	1.14904	59.8364	94.44	94.13	Suggested
Quadratic	1.22456	73.3972	93.52	92.84	
Full cubic	1.21462	62.3793	93.62	92.26	
Full quartic	1.21111	86.3057	93.05	92.23	
Transmittance					
Linear	4.79487	983.071	68.44	66.69	
Quadratic	1.97902	178.68	95.07	94.33	Suggested
Full cubic	1.337	103.393	93.02	92.41	
Full quartic	1.38986	113.005	93.56	92.72	

SE: Standard error of the regression, represents the standard distance between the data values and fitted regression line. PRESS: Prediction error sum of squares, the smaller the PRESS value, the better the model predictive ability. R<sup>2</sup>: Percentage of response variable variation; the higher the value, the better the model fits the data. R<sup>2</sup> (adj): Percentage of response variable variation based on its relationship with one or more predictor variables, LCT-SMEDS: Long-chain triglyceride-self-microemulsifying delivery system, AST: Astaxanthin, PDI: Polydispersity index

was increased, the self-microemulsion droplet size might be dramatically reduced but not homogeneously so that the PDI value of the system would be raised. In Figures 2 and 3, the response surface and contour plots for PDI ( $Y_2$ ) obtained from the AST LCT-SMEDS formulations were respectively presented.

#### Influence on zeta potential ( $Y_3$ )

The overall charges presented on the surface of microemulsion droplets can be described by the value of zeta potential. The repulsive electrostatic forces, which reduce possibility of particle aggregation, are exhibited by a high zeta potential value ( $> +30$  mV or  $< -30$  mV).<sup>[50,51]</sup> In general, the greater the zeta potential of an emulsion droplet, the higher the probability of resulting in a relatively more physically stable system. It was commonly observed that the negative charges on the surfaces of microemulsion droplets were found in conventional SMEDS formulations as free fatty acids were presented on oil globules. Table 2 described the zeta potential measurement results of all AST LCT-SMEDS formulations diluted with deionized water. In general, the values of zeta potential ranged from  $-12.90$  mV to  $-8.34$  mV, which indicated that our AST-loaded SMEDS was fairly stabilized. However, no aggregation or phase separation

of the microemulsions resulted from all SMEDS formulations were observed within 24 h.

According to Losso *et al.*,<sup>[52]</sup> it was reported that the shelf-life stability of most emulsions was associated with their surface properties. However, Roland *et al.*<sup>[53]</sup> found insignificant correlation between zeta potential and overall physical stability, and in their case visually observed stable microemulsions exhibited moderate zeta potential values which were similar to our results. Other factors including a decrease in the microemulsion droplet size might also play a critical role in stabilizing the system. It was reported that absorption of colloidal delivery systems such as nanoparticles and nano/microemulsions through the GI tract was enhanced by the charge-dependent interaction with mucus and cell membrane barriers.<sup>[54]</sup> The thin layer of mucus acted as a strong barrier for penetration of a substance. Due to electrostatic interactions, positively charged particles were hindered from diffusing into deeper mucus regions by the negatively charged mucus gel. On the contrary, the negatively charged particles were shown to permeate more easily into the mucus gel layer and got absorbed more efficiently through the GI cell membranes than the positively charged ones.

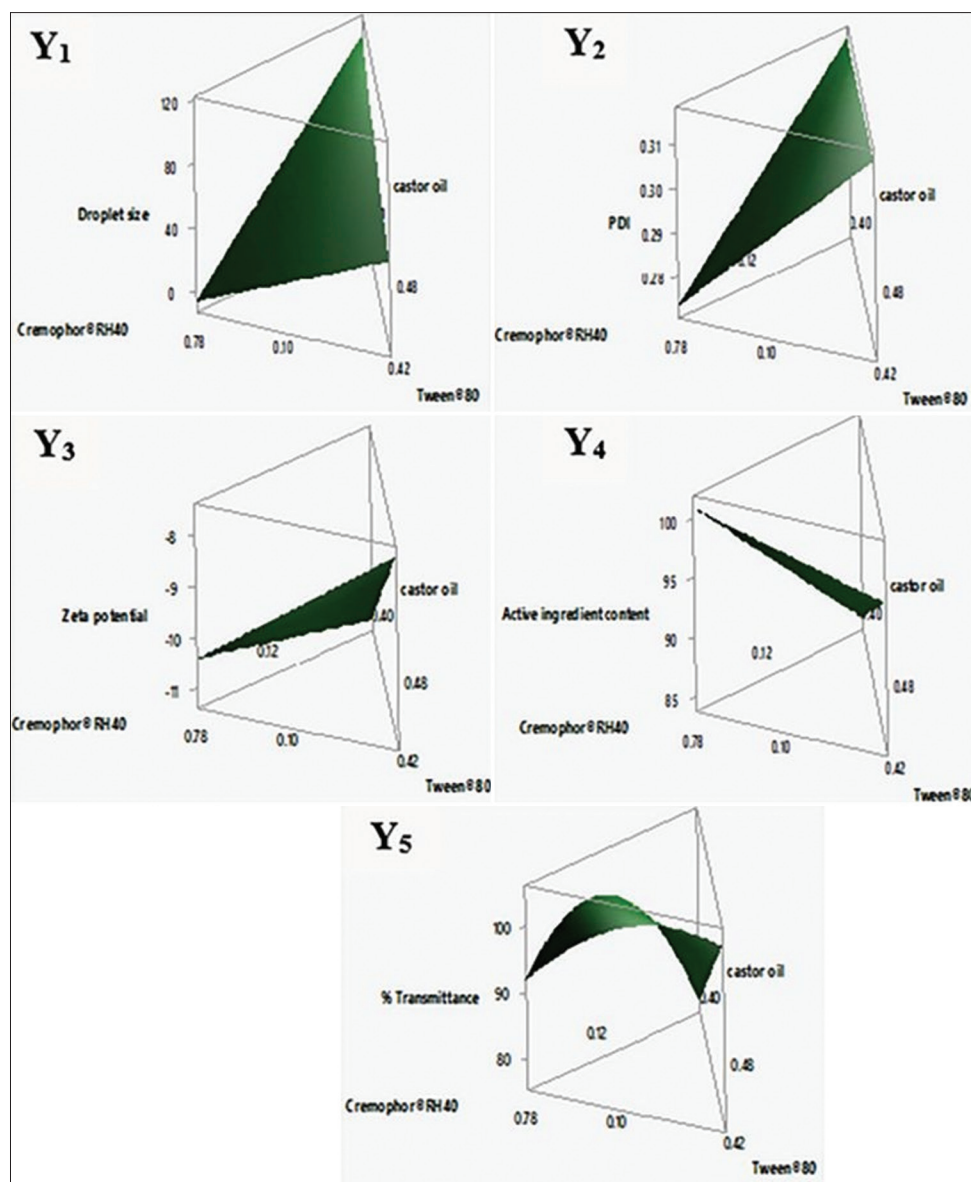


**Figure 2:** Three-dimensional response surface plots for the effects of the independent variables on the responses: droplet size ( $Y_1$ ), polydispersity index ( $Y_2$ ), zeta potential ( $Y_3$ ), active ingredient content ( $Y_4$ ), and percent transmittance ( $Y_5$ ) of the astaxanthin long-chain triglyceride-self-microemulsifying delivery system formulations

Although a quadratic model was suggested to the zeta potential data of AST SMEDS formulas with the largest  $R^2$  and adjusted  $R^2$  values [Table 3], after performing the regression analysis the interaction terms in the quadratic model were found to be statistically insignificant (data not shown) and the prediction model for  $Y_3$  was reduced and simplified to a linear equation as follows.

$$\text{Zeta potential } (Y_3) = -13.79 X_1 - 11.32 X_2 - 1.88 X_3 \quad (4)$$

From Eq. (4), the absolute values of the coefficients of the main factors were in the order of  $X_1 > X_2 \gg X_3$ . According to observation from the equation, an increase in the quantities of oil, surfactant, and cosurfactant may direct towards a decrease in the zeta potential. It could be summarized from the  $P < 0.05$  [Table 4] that zeta potential was significantly affected by all the individual terms. An impact on the zeta potential value

of microemulsions was most probably related to the type and the electrostatic nature of the ingredients. Among the three compositions, the amount of an oil phase ( $X_1$ ) had the most substantial effect on the zeta potential as it might possess some free fatty acids contributing to the negative charges on the microemulsion droplet surfaces. The plots in Figures 2 and 3 presented a linear relationship between the independent variables and zeta potential ( $Y_3$ ) showing the response surface and the contour region, respectively.

Influence on active ingredient content ( $Y_4$ )

Since loading capacity of the SMEDS formulation affected the number of the final dose in a dosage form, the active ingredient content was selected as one of the criteria for the preparation optimization. Higher loading efficiency of the SMEDS led to an equivalent lower dose of a compound to be delivered and a minimized amount of oils and surfactants/

**Table 4:** Summary of the analysis of variance results of the measured responses ( $Y_n$ ) of the AST LCT-SMEDS formulations.

Response	Source	DF	Seq SS	Adj SS	Adj MS	F-value	P-value
Droplet size ( $Y_1$ )	Regression	5	53988.600	53988.600	10797.700	101.610	<0.0001
	Linear	2	46223.200	7527.500	3763.700	35.420	<0.0001
	Quadratic	3	7765.400	7765.400	2588.500	24.360	<0.0001
	$X_1X_2$	1	7083.100	7068.400	7068.400	66.510	<0.0001
	$X_1X_3$	1	47.300	679.000	679.000	6.390	0.016
	$X_2X_3$	1	635.000	635.000	635.000	5.980	0.020
	Residual Error	33	3506.900	3506.900	106.300		
	Lack-of-Fit	7	896.300	896.300	128.000	1.280	0.301
	Pure Error	26	2610.600	2610.600	100.400		
Total	38	57495.500	0.650				
PDI ( $Y_2$ )	Regression	2	0.006	0.006	0.003	0.650	0.030
	Linear	2	0.006	0.006	0.003	0.650	0.030
	Residual Error	36	0.171	0.171	0.004		
	Lack-of-Fit	10	0.104	0.104	0.010	4.040	0.102
	Pure Error	26	0.067	0.067	0.002		
	Total	38	0.177				
Zeta potential ( $Y_3$ )	Regression	2	4.515	4.515	2.257	0.450	0.041
	Linear	2	4.515	4.515	2.257	0.450	0.041
	Residual Error	36	180.718	180.718	5.020		
	Lack-of-Fit	10	73.671	73.671	7.367	1.790	0.113
	Pure Error	26	107.046	107.046	4.117		
	Total	38	185.233				
Active ingredient content ( $Y_4$ )	Regression	2	917.520	917.520	458.762	305.930	<0.0001
	Linear	2	917.520	917.520	458.762	305.930	<0.0001
	Residual Error	36	53.980	53.980	1.500		
	Lack-of-Fit	10	15.630	15.630	1.563	1.060	0.426
	Pure Error	26	38.360	38.360	1.475		
	Total	38	971.510				
Transmittance ( $Y_5$ )	Regression	5	2493.44	2493.44	623.360	163.68	<0.0001
	Linear	2	1795.25	1270.62	635.309	166.82	<0.0001
	Quadratic	3	698.19	698.19	349.093	91.67	<0.0001
	$X_1X_2$	1	344.66	344.66	344.665	175.86	<0.0001
	$X_1X_3$	1	344.66	344.66	344.665	175.86	<0.0001
	$X_2X_3$	1	8.86	8.86	8.863	2.33	0.136
	Residual Error	34	129.48	129.48	3.808		
	Lack-of-Fit	8	79.26	79.26	9.907	5.13	0.001
	Pure Error	26	50.22	50.22	1.932		
	Total	38	2622.92				

DF: Degrees of freedom, Seq SS: Sequential sums of squares, Adj SS: Adjusted sums of squares, Adj MS: Adjusted mean square, LCT-SMEDS: Long-chain triglyceride-self-microemulsifying delivery system, AST: Astaxanthin, PDI: Polydispersity index

cosurfactants used. It was observed that a large quantity of a surfactant/cosurfactant caused the irritation on the GI tract; however, the amount of surfactants/cosurfactants incorporated in the SMEDS preparation may be lessened at the maximum active ingredient loading.<sup>[36]</sup> The AST contents entrapped in the LCT-SMEDS formulations ranged from 84.55% to 99.71% as listed in Table 2, indicating a remarkably

high loading capacity of all thirteen self-microemulsifying system preparations. According to the statistically fitted data, the software suggested a linear model with high values of  $R^2$  and adjusted  $R^2$  for AST LCT-SMEDS [Table 3]. To confirm the relationship between independent variables and AST content in LCT-SMEDS formulations, Eq. (5) was generated on the basis of the outcomes of analysis of variance in Table 4.

Active ingredient

$$\text{content } (Y_4) = 53.96 X_1 + 108.13 X_2 + 93.89 X_3 \quad (5)$$

As can be noticed from the positive values of all coefficients in the above equation, increases in the amounts of Cremophor® RH 40, Tween® 80, and castor oil would enhance the amount of AST loaded in SMEDS. This was possibly contributed to the fact that the active substance had high solubilities in all ingredients. Furthermore, significance of the main factors was in the order of  $X_2 > X_3 \gg X_1$ , and an appropriate combination of a surfactant plus a cosurfactant accounted for this particularly high loading capacity of AST in this delivery system. The 3D response surface and contour plots for the active ingredient AST in the LCT-SMEDS were illustrated in Figures 2 and 3, respectively, to additionally support the obtained Eq. (5).

Influence on transmittance ( $Y_5$ )

Micro- or nano-emulsion formation could be confirmed by transparency, and thus the percentage of transmittance

through the product was selected as another important response in this work. It was studied that high clarity of microemulsions was indicated by a transmittance value  $\geq 98\%$ .<sup>[55]</sup> The transparency of microemulsions could be reduced by a larger particle size. As shown in Table 2, the transmittance of the AST-loaded microemulsions produced from the LCT-SMEDS formulations ranged between 75.72% and 98.57%. Most of the AST SMEDS formulations could be measured transmittance  $>90\%$  implying visually clear microemulsions while only three formulas (i.e., LCT-SMEDS<sub>1,4,5</sub>) were off slightly low clarity and possessed less percent transmittance values because they consisted of high amounts of castor oil in the formulations. The suggested quadratic model with the highest  $R^2$  and adjusted  $R^2$  in Table 3 was statistically fitted well to the percentage transmittance data of the formed AST microemulsions. The effects of independent variables on percent transmittance of the AST LCT-SMEDS formulations were reflected by the following Eq. (6).

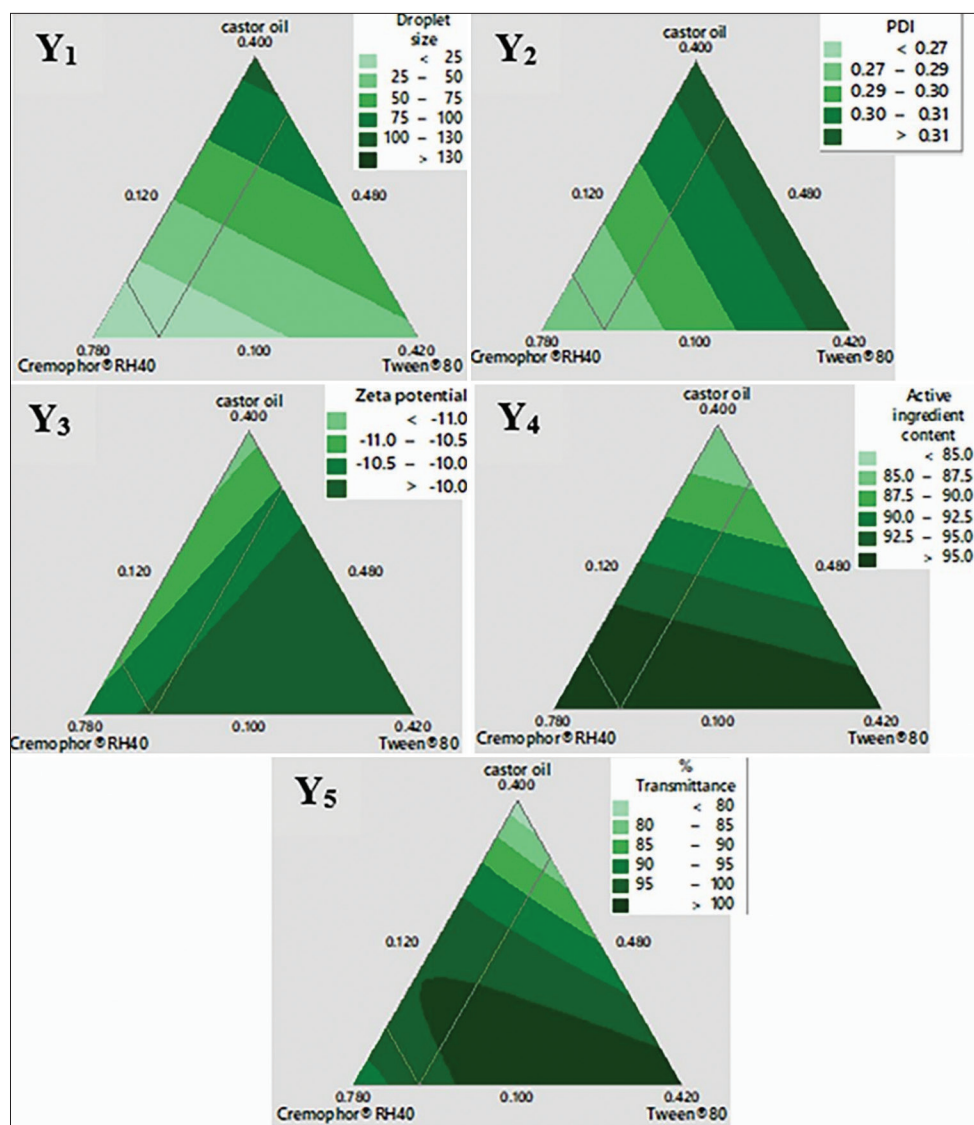


**Figure 3:** Contour plots for the effects of the independent variables on the responses: droplet size ( $Y_1$ ), polydispersity index ( $Y_2$ ), zeta potential ( $Y_3$ ), active ingredient content ( $Y_4$ ), and percent transmittance ( $Y_5$ ) of astaxanthin long-chain triglyceride-self-microemulsifying delivery system formulations

$$\text{Transmittance } (Y_5) = -228.2 X_1 + 42.3 X_2 + 60.1 X_3 + 658.8 X_1 X_2 + 354.8 X_1 X_3 + 243.7 X_2 X_3 \quad (6)$$

In the above equation, the order of the absolute values of the main effect coefficients was  $X_1 \gg X_3 > X_2$ . The percentage transmittance may be reduced by an enhancement in the amount of the oil phase and may be improved with increases in the quantities of the cosurfactant/surfactant in a formula. The effects of the related factors and their interactions on the percent transmittance ( $Y_5$ ) were found to be significant with the  $P < 0.05$  as shown in Table 4. It can be summarized from Eq. 6 that the interaction terms  $X_1 X_2$ ,  $X_1 X_3$ , and  $X_2 X_3$  had an essentially synergistic effect on the percentage of transmittance as expressed by the positive coefficient values; while, the interaction between castor oil and Cremophor® RH 40 ( $X_1 X_2$ ) seemed to have the most impact on  $Y_5$  compared to other interaction terms  $X_1 X_3$  and  $X_2 X_3$ . Figures 2 and 3 depicted the 3D curvilinear response surface and contour plots, respectively, for the AST LCT-SMEDS formulations indicating the effects of excipients on transmittance ( $Y_5$ ) of the formed microemulsions.

#### Optimization and validation of the AST SMEDS formulation

After the influences of the input variables on the responses have been thoroughly studied in the earlier sections, optimization of the amounts of the three components in a formulation was further performed. The AST LCT-SMEDS formulas were optimized to determine the degrees of the independent variables ( $X_1$ ,  $X_2$ , and  $X_3$ ) that would aim to provide minimum values of the droplet size ( $Y_1$ ) and PDI ( $Y_2$ ) with maximum absolute values of zeta potential ( $Y_3$ ), AST content ( $Y_4$ ), and percent transmittance ( $Y_5$ ) with consideration of the desirability function. The effects of the optimized input variables on the observed responses were examined from the polynomial equation, response optimizer plot, and overlaid contour plot. After consolidating all the equations expressed above, the levels of independent variables of the optimized SMEDS formulation (denoted as LCT-SMEDS<sub>OTM</sub> in our study) were suggested by the response optimizer plot in Minitab™ with an overall desirability value of 0.8074. The overlaid contour plot of the optimized AST LCT-SMEDS formulation taking into account all output properties within the desired ranges was presented in Figure 4. The optimized excipient ratio of  $X_1$ ,  $X_2$ , and  $X_3$  for the AST LCT-SMEDS formulation was 19.59%, 62.34%, and 18.03%, respectively, which would theoretically provide the values of 22.71 nm, 0.28, -9.70 mV, 97.88%, and 98.39% for  $Y_1$ ,  $Y_2$ ,  $Y_3$ ,  $Y_4$ , and  $Y_5$ , respectively.

To validate the mixture design model, microemulsion containing AST from the optimized SMEDS formulation was then prepared, and the values of experimentally measured responses were compared with the values predicted from the program. Reliability and accuracy of the estimation using the desirability functions were evaluated by calculating prediction errors. If the measured values were close to their predicted values, the prediction error would be small suggesting that the experimental mixture design successfully optimized the AST LCT-SMEDS formulation. Table 5 listed the predicted and measured values of  $Y_1$  to  $Y_5$  for the optimized AST LCT-SMEDS<sub>OTM</sub> formula and the calculated percentage of prediction errors. All the responses data experimentally measured from

the actual self-microemulsions obtained were generally in extremely close agreement with the expected values computed by Minitab™ software. The prediction errors of all responses were very small (<4%) and considered to be desirable as shown in Table 5. Therefore, it could be concluded from the results of these observations that the mixture design method applied for the optimization of AST-loaded self-microemulsions in our research was exceptionally reliable and accurate. However, the optimized formulation and its physicochemical attributes were subjected to the choices of excipients selected (i.e., material dependent) and will need further studies.

## Performance Characterization of the Optimized AST SMEDS Formulation

Performance of the optimized AST-loaded castor oil-based self-microemulsifying system (LCT-SMEDS<sub>OTM</sub>) was evaluated in the following aspects: Physical properties (including visual observation, self-emulsification time, and refractive index), emulsion droplet morphology, physicochemical stability, and *in vitro* release profiles of AST from the optimized formulation.

#### Physical property studies

Identification of any signs of phase separation or precipitation of the optimized formulation was visually performed after dilution. With the help of visibility grading criteria, SMEDS

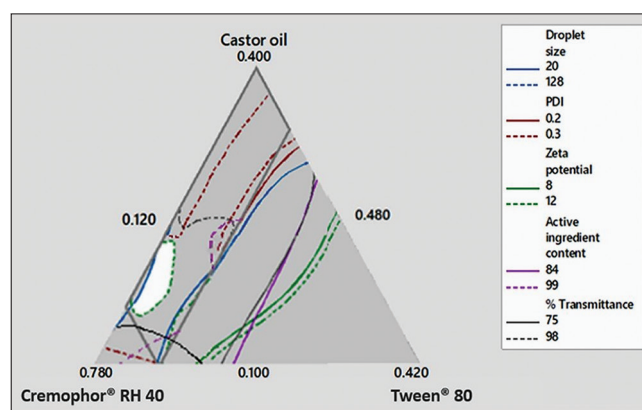


**Figure 4:** An overlaid contour plot for the optimized astaxanthin long-chain triglyceride-self-microemulsifying delivery system formulation

**Table 5:** Predicted and measured ( $n=3$ ) values of the optimized AST LCT-SMEDS formulation and the percentage prediction errors of responses

Responses	Predicted value	Measured value	Prediction error (%)
Droplet size ( $Y_1$ ; nm)	22.71	22.55 ± 0.96	-0.70
PDI ( $Y_2$ )	0.28	0.27 ± 0.02	-3.70
Zeta potential ( $Y_3$ ; mV)	-9.70	-9.35 ± 1.75	-3.74
Active ingredient content ( $Y_4$ ; %)	97.88	96.49 ± 0.60	-1.44
Transmittance ( $Y_5$ ; %)	98.39	98.80 ± 0.11	0.41

LCT-SMEDS: Long-chain triglyceride-self-microemulsifying delivery system, AST: Astaxanthin, PDI: Polydispersity index

formulations examined were usually graded from A to E.<sup>[56]</sup> The definitions of each class in the visual grading system were provided in Section 2.2.8. When SMEDS was dispersed in an aqueous phase,  $S_{\text{mix}}$  was assumed to penetrate the aqueous phase and redistribute between the oil-water interfaces<sup>[39]</sup> resulting in clear, fast self-forming (grade A) to milky, poor or non-forming (grade E) microemulsions. According to a visual observation, the optimized AST LCT-SMEDS<sub>OTM</sub> formulation was noticed with no indications of precipitation and phase separation. Clear and transparent microemulsions were rapidly formed through this optimized formula and hence classified as the grade A shown in Table 6. A refractive index of the obtained self-microemulsions from the optimized formula was also measured. The refractive index result, approximately equal to 1.422, was shown in Table 6. It was examined that there was no significant difference in the refractive index data of the optimized formulation measured. The result of refractive index was reasonably close to the value of water showing the optimized formulation was transparent in nature and confirming the grade A visibility result of the physical appearance classification.

Emulsification time was also determined for the optimized AST SMEDS formulation. Self-emulsification means that a SMEDS formulation has to be rapidly dispersed by a gentle agitation when diluted with water. Determining the emulsification rate could estimate the efficiency of self-emulsification. The optimized AST-loaded self-microemulsifying formulation possessed the emulsification time of faster than 1 min (44 s) indicating a good self-emulsification efficiency as reported in Table 6.

#### Size and shape of the self-microemulsion droplets

As described earlier, the appearance of the optimized AST SMEDS formulation was homogeneous and transparent liquid. The morphology of microemulsions obtained from AST LCT-SMEDS<sub>OTM</sub> was further observed using TEM. The transmission electron micrographs of the diluted AST LCT-SMEDS<sub>OTM</sub> self-microemulsions were shown in Figure 5. It can be observed that the oil droplets (noticed by darker color spots of AST) were typically <25 nm in size and homogeneously dispersed in the external aqueous phase with good integrity indicating that o/w microemulsions were successfully formed. Moreover, it was determined that no signs of AST precipitation from the LCT-SMEDS<sub>OTM</sub> were noticed suggesting the good stability of the diluted AST LCT-SMEDS<sub>OTM</sub> self-microemulsion system.

#### Stability studies

In addition, the freezing-thawing tests throughout the cycles from -20°C to 25°C were performed on self-assembling microemulsions obtained from the optimized AST LCT-SMEDS formulation. The droplet size, PDI, zeta potential, and AST content in the self-microemulsions were determined immediately before the study and after three cycles. As shown

in Table 7, the data obtained after each cycle of freezing-thawing were similarly close to those from the LCT-SMEDS<sub>OTM</sub> formulation before the test. Although after each freeze-thaw cycle the emulsion droplet size was slightly enlarged and a little more broadly distributed as well as the AST amount was gradually reduced, there were statistically unimportant. However, no significant changes in physical appearance of the diluted self-microemulsions were observed after freeze-thaw stability studies. Moreover, the diluted microemulsions indicated no signs of AST precipitation, phase separation, cracking, or creaming after being subjected to the freezing-thawing cycles, which suggested the formation of remarkably stable microemulsions from the LCT-SMEDS<sub>OTM</sub> formulation. The self-microemulsion droplets remained stable with AST contents of over 95% after three cycles of the freeze-thaw stability study. Nevertheless, these LCT-SMEDS<sub>OTM</sub> stability results were collected through the freezing-thawing cycles during a short period of time only. A long-term stability study on microemulsions obtained from the optimized AST LCT-SMEDS formulation might be needed in the future work.

#### In vitro release studies

Release of AST from the optimized AST LCT-SMEDS<sub>OTM</sub> formulation was studied with the use of dialysis bag method explained in Section 2.2.13 and compared to one marketed preparation and raw material AST powder. The *in vitro* release profiles of AST from the LCT-SMEDS<sub>OTM</sub> formulation, a marketed preparation, and a raw material of the same AST amount in sequentially changing different media over time were illustrated in Figure 6. At pH = 1.2, the amount of AST released from the optimized LCT-SMEDS was higher than 40% after the first 30 min while approximately 80% of AST was released after 2 h at pH = 4.5. AST release from LCT-SMEDS<sub>OTM</sub> was successfully completed and gradually approached a plateau level within 4 h in pH = 7.4, and the cumulative amount dissolved of AST resulted in an average value of 93.09% after sustaining for 8 h. This might be related to the formation of small microemulsion droplets, their rapid dispersion, and thus better release rate due to greater solubility of AST in the excipients of SMEDS.<sup>[57,58]</sup> In addition, the oil phase of SMEDS may be the factor enhancing the release because it may serve as carrier molecules for active compound molecules to diffuse through a dialysis membrane.<sup>[35,40,59]</sup> The overall dissolution rate of the optimized LCT-SMEDS formulation represented by >90% of AST released could postulate the availability of AST at the site of absorption. Moreover, the dissolution profiles showed that the percentages of AST released from the LCT-SMEDS<sub>OTM</sub> formulation were significantly larger than those from the marketed preparation and the AST raw material over an 8-h period. The dissolution data showed that the release rates of AST were distinctly reduced for the commercial product and the raw material; the cumulative AST released from the marketed dosage form was merely within 20–40%

**Table 6:** Results of the physical property testing of the optimized AST LCT-SMEDS formulation. Self-emulsification time and refractive index were measured in triplicate

Visibility grade	Precipitation	Phase separation	Self-emulsification time (s)	Refractive index
A	No	No	44 ± 1	1.4222 ± 0.07

LCT-SMEDS: Long-chain triglyceride-self-microemulsifying delivery system, AST: Astaxanthin

**Table 7:** Stability profiles of the optimized AST LCT-SMEDS formulation ( $n=3$ )

Treatment	Droplet size (nm)	PDI	Zeta potential (mV)	AST content (%)
Before test	22.55±0.96	0.25±0.02	-11.35±1.75	96.49±0.60
Freeze-thaw (1 <sup>st</sup> cycle)	22.96±0.84	0.27±0.02	-12.37±1.49	96.00±0.56
Freeze-thaw (2 <sup>nd</sup> cycle)	23.50±0.63	0.28±0.02	-12.55±1.59	95.82±0.71
Freeze-thaw (3 <sup>rd</sup> cycle)	23.67±0.67	0.29±0.02	-13.19±1.27	95.54±0.69

LCT-SMEDS: Long-chain triglyceride-self-microemulsifying delivery system, AST: Astaxanthin, PDI: Polydispersity index

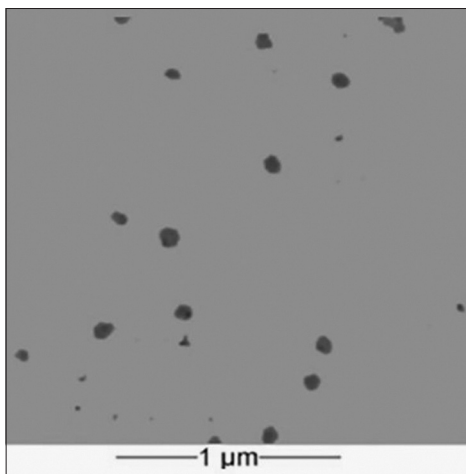


**Figure 5:** Transmission electron microscopy images of the optimized astaxanthin-loaded castor oil-based self-microemulsifying delivery system formulation

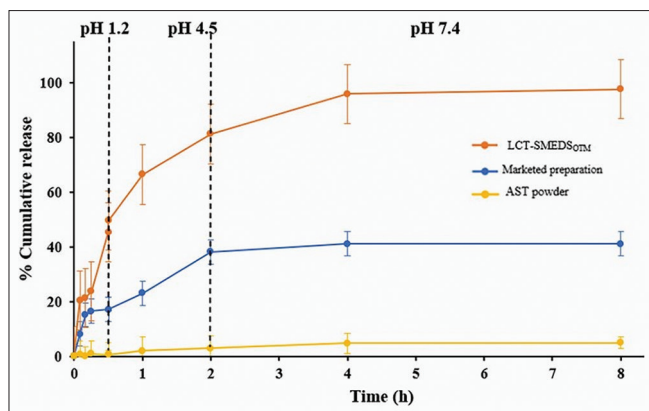


**Figure 6:** Astaxanthin (AST) release profiles ( $n=3$ ) from the optimized formulation (long-chain triglyceride-self-microemulsifying delivery system<sub>OTM</sub>) compared to a marketed preparation and raw material AST powder in sequentially changing dissolution media: pH 1.2 for 0.5 h, pH 4.5 for 1.5 h, and pH 7.4 for 6 h

and from the unprocessed powder was even very low (approximately not more than 5%) during 8 h. Depending on brands, commercial products available in the market usually contained <2–12 mg of AST dissolved in oil vehicles such as vegetable or krill oils filled in soft gelatin capsules. Regardless of the dose per unit, some commercial products still had the low aqueous solubility and bioavailability issues. Our results showed that the LCT-SMEDS formulations could rapidly increase the dissolution rate and significantly enhanced the release of AST thus exhibited better bioavailability and

efficacy compared to the marketed preparation and untreated AST powder.

## CONCLUSIONS

In this study, an optimized AST-loaded SMEDS formulation was successfully developed using the mixture design. The optimized SMEDS formulation included 19.59% castor oil (lipid phase;  $X_1$ ), 62.34% Cremophor® RH 40 (surfactant;  $X_2$ ), and 18.03% Tween® 80 (cosurfactant;  $X_3$ ). Good agreement was observed between the model predicted outputs and the experimentally measured values of the droplet size ( $Y_1$ ), PDI ( $Y_2$ ), zeta potential ( $Y_3$ ), active ingredient content ( $Y_4$ ), and percentage of transmittance ( $Y_5$ ). Moreover, from the results of visual observation, self-emulsification time, refractive index, TEM, and freeze-thaw stability studies, it could be concluded that rapidly forming microemulsions with good physicochemical properties and stability were generated by the optimized LCT-SMEDS formulation. *In vitro* release studies of the optimized AST-loaded SMEDS showed that the release of the active substance was over 90% within 4 h. Our optimized AST LCT-SMEDS formula was proved to be superior to the commercial product and raw AST powder with respect to the *in vitro* dissolution profiles. The effects of other types of materials used in the SMEDS formulations on quality attributes of the self-microemulsions can be further investigated. In addition, future work regarding evaluations of cell permeability, *in vivo* bioavailability, and adverse effect of the LCT-SMEDS containing AST for oral administration should be conducted after this current study. Our optimized AST-loaded castor oil-based SMEDS could be potentially turned to be a new and commercially feasible formulation of AST with enhanced dissolution and release properties. We ultimately hope that this novel AST self-microemulsifying platform can be a future candidate for effectively delivering the biologically active substance to target cells in the body and ultimately that this AST SMEDS product will be able to beneficially help mitigating symptoms in elderly patients undergoing with neurodegenerative diseases.

## ACKNOWLEDGMENTS

This research was funded by Chulalongkorn University. The researchers would like to gratefully thank the Grants for Development of New Faculty Staff, Ratchadaphiseksomphot Endowment Fund, Chulalongkorn University (Contract Number: CU-GR\_62\_001\_33\_001-T). The research fund granted from the Graduate Program of Pharmaceutical Sciences and Technology, Faculty of Pharmaceutical Sciences, Chulalongkorn University was also acknowledged. The researchers want to thank Professor Dr. Garnpimol C.

Ritthidej, Ms. Wai Thet Aung, scientific staffs, and technicians of the Department of Pharmaceutics and Industrial Pharmacy, Faculty of Pharmaceutical Sciences, Chulalongkorn University for their laboratory assistance. The authors would like to thank the Pharmaceutical Research Instrument Center of the Faculty of Pharmaceutical Sciences and the Scientific and Technological Research Equipment Centre of Chulalongkorn University for providing research instruments. One of the authors, Ms. M. M. K. Zin, also would like to acknowledge the Scholarship Program for ASEAN Countries granted from the Office of Academic Affairs, Chulalongkorn University for the financial support during her master's degree study.

## REFERENCES

- Guerin M, Huntley M E, Olaizola M. *Haematococcus* astaxanthin: Applications for human health and nutrition. Trends Biotechnol 2003;21:210-6.
- Miki W. Biological functions and activities of animal carotenoids. Pure Appl Chem 1991;63:141-6.
- Dufossé L, Pigments from microalgae and microorganisms: Sources of food colorants. In: Socaciu C, Sikorski ZE, editors. Food Colorants, Chemical and Functional Properties. Boca Raton, Florida: CRC Press. 2008. p. 399-426.
- Galasso C, Orefice I, Pellone P, Cirino P, Miele R, Ianora A, *et al.* On the neuroprotective role of astaxanthin: New perspectives? Mar Drugs 2018;16:247.
- Grimmig B, Kim SH, Nash K, Bickford PC, Shytle RD. Neuroprotective mechanisms of astaxanthin: A potential therapeutic role in preserving cognitive function in age and neurodegeneration. Geroscience 2017;39:19-32.
- Martínez-Álvarez Ó, Calvo MM, Gómez-Estaca J. Recent advances in astaxanthin micro/nanoencapsulation to improve its stability and functionality as a food ingredient. Mar Drugs 2020;18:406.
- Higuera-Ciapara I, Félix-Valenzuela L, Goycoolea FM. Astaxanthin: A review of its chemistry and applications. Crit Rev Food Sci Nutr 2006;46:185-96.
- Pan L, Wang H, Gu K. Nanoliposomes as vehicles for astaxanthin: Characterization, *in vitro* release evaluation and structure. Molecules 2018;23:2822.
- Guan L, Liu J, Yu H, Tian H, Wu G, Liu B, *et al.* Water-dispersible astaxanthin-rich nanopowder: preparation, oral safety and antioxidant activity *in vivo*. Food Funct 2019;10:1386-97.
- Zhang P, Liu Y, Feng N, Xu J. Preparation and evaluation of self-microemulsifying drug delivery system of oridonin. Int J Pharm 2008;355:269-76.
- Shah N, Carvajal M, Patel C, Infeld MH, Malick AW. Self-emulsifying drug delivery systems (SEDDS) with polyglycolized glycerides for improving *in vitro* dissolution and oral absorption of lipophilic drugs. Int J Pharm 1994;106:15-23.
- Charman SA, Charman WN, Rogge MC, Wilson TD, Dutko FJ, Pouton CW. Self-emulsifying drug delivery systems: Formulation and biopharmaceutical evaluation of an investigational lipophilic compound. Pharm Res 1992;9:87-93.
- Thongrangsali S, Phaechamud T, Lipipun V, Ritthidej GC. Bromocriptine tablet of self-microemulsifying system adsorbed onto porous carrier to stimulate lipoproteins secretion for brain cellular uptake. Colloid Surface B Biointerfaces 2015;131:162-9.
- Lamaisakul S, Tantituvanont A, Lipipun V, Ritthidej G. Development of novel cationic microemulsion as parenteral adjuvant for influenza vaccine. Asian J Pharm Sci 2020;15:591-604.
- Yu L X, Amidon G, Khan MA, Hoag SW, Polli J, Raju GK, *et al.* Understanding pharmaceutical quality by design. AAPS J 2014;16:771-83.
- Zhang L, Mao S. Application of quality by design in the current drug development. Asian J Pharm Sci 2017;12:1-8.
- Mishra V, Thakur S, Patil A, Shukla A. Quality by design (QbD) approaches in current pharmaceutical set-up. Expert Opin Drug Deliv 2018;15:737-58.
- Bhattacharya S, Mishra S, Prajapati BG. Design and development of docetaxel solid self-microemulsifying drug delivery system using principal component analysis and d-optimal design. Asian J Pharm 2018;12:122-44.
- Sandhu P S, Kumar R, Beg S, Jain S, Kushwah V, Katare OP, *et al.* Natural lipids enriched self-nano-emulsifying systems for effective co-delivery of tamoxifen and naringenin: systematic approach for improved breast cancer therapeutics. Nanomed Nanotechnol Biol Med 2017;13:1703-13.
- Köksoy O. A nonlinear programming solution to robust multi-response quality problem. Appl Math Comput 2008;196:603-12.
- Singh D, Tiwary AK, Bedi N. Canagliflozin loaded SMEDDS: Formulation optimization for improved solubility, permeability and pharmacokinetic performance. J Pharm Investig 2019;49:67-85.
- Li Z, Cho B R, Melloy B J. Quality by design studies on multi-response pharmaceutical formulation modeling and optimization. J Pharm Innov 2013;8:28-44.
- Zin MM, Boonkanokwong V. Development and characterization of astaxanthin-loaded self-microemulsifying delivery system. In: Suksaeree J, Shuwisitkul D, editors. Pathum Thani, Thailand: The International Conference and Exhibition on Pharmaceutical Sciences and Technology 2020 (PST2020), College of Pharmacy, Rangsit University, College of Pharmacy, Rangsit University; 2020. p. 37-49.
- Qureshi MJ, Mallikarjun C, Kian WG. Enhancement of solubility and therapeutic potential of poorly soluble lovastatin by SMEDDS formulation adsorbed on directly compressed spray dried magnesium aluminometasilicate liquid loadable tablets: A study in diet induced hyperlipidemic rabbits. Asian J Pharm Sci 2015;10:40-56.
- Rivera S, Canela R. Influence of sample processing on the analysis of carotenoids in maize. Molecules 2012;17:11255-68.
- Shanmugapriya K, Kim H, Saravana PS, Chun BS, Kang HW. Astaxanthin-alpha tocopherol nanoemulsion formulation by emulsification methods: Investigation on anticancer, wound healing, and antibacterial effects. Colloid Surface B 2018;172:170-9.
- Singh AK, Chaurasiya A, Awasthi A, Mishra G, Asati D, Khar RK, *et al.* Oral bioavailability enhancement of exemestane from self-microemulsifying drug delivery system (SMEDDS). AAPS PharmSciTech 2009;10:906-16.
- Khoo SM, Humberstone AJ, Porter CJ, Edwards GA, Charman WN. Formulation design and bioavailability assessment of lipidic self-emulsifying formulations of halofantrine. Int J Pharm 1998;167:155-64.
- Shen H, Zhong M. Preparation and evaluation of self-microemulsifying drug delivery systems (SMEDDS) containing atorvastatin. J Pharm Pharmacol 2006;58:1183-91.
- Yang R, Huang X, Dou J, Zhai G, Su L. Self-microemulsifying drug delivery system for improved oral bioavailability of oleanolic acid: Design and evaluation. Int J Nanomed 2013;8:2917-2926.
- Kassem AA, Mohsen AM, Ahmed RS, Essam TM. Self-nanoemulsifying drug delivery system (SNEDDS) with enhanced solubilization of nystatin for treatment of oral candidiasis: Design, optimization, *in vitro* and *in vivo* evaluation. J Mol Liq 2016;218:219-232.
- Agrawal AG, Kumar A, Gide PS. Self-emulsifying drug delivery system for enhanced solubility and dissolution of glipizide. Colloid Surface B Biointerfaces 2015;126:553-60.
- Deshmukh A, Kulkarni S. Solid self-microemulsifying drug delivery system of ritonavir. Drug Dev Ind Pharm 2014;40:477-87.
- Chuog MC, Christensen JM, Ayres JW. New dissolution method for mesalamine tablets and capsules. Dissolution Technol

- 2008;15:7-14.
35. Sha X, Yan G, Wu Y, Li J, Fang X. Effect of self-microemulsifying drug delivery systems containing Labrasol on tight junctions in Caco-2 cells. *Eur J Pharm Sci* 2005;24:477-86.
  36. Prajapat MD, Patel NJ, Bariyac A, Patel SS, Butani S. Formulation and evaluation of self-emulsifying drug delivery system for nimodipine, a BCS Class II drug. *J Drug Deliv Sci Tech* 2017;39:59-68.
  37. Constantinides PP. Lipid microemulsions for improving drug dissolution and oral absorption: Physical and biopharmaceutical aspects. *Pharm Res* 1995;12:1561-72.
  38. Lawrence MJ, Rees GD. Microemulsion-based media as novel drug delivery systems. *Adv Drug Del Rev* 2000;45:89-121.
  39. Patel AR, Vavia PR. Preparation and *in vivo* evaluation of SMEDDS (self-microemulsifying drug delivery system) containing fenofibrate. *AAPS J* 2007;9:344-52.
  40. Dixit AR, Rajput SJ, Patel SG. Preparation and bioavailability assessment of SMEDDS containing valsartan. *AAPS PharmSciTech* 2010;11:314-21.
  41. Basalious EB, Shawky N, Badr-Eldin SM. SNEDDS containing bioenhancers for improvement of dissolution and oral absorption of lacidipine. I: Development and optimization. *Int J Pharm* 2010;391:203-11.
  42. Zeng L, Xin X, Zhang Y. Development and characterization of promising Cremophor EL-stabilized o/w nanoemulsions containing short-chain alcohols as a cosurfactant. *RSC Adv* 2017;7:19815-27.
  43. Rachmawati H, Novel MA, Ayu S, Berlian G, Tandrasasmita OM, Tjandrawinata RR, *et al.* The *in vitro in vivo* safety confirmation of PEG-40 hydrogenated castor oil as a surfactant for oral nanoemulsion formulation. *Sci Pharm* 2017;85:18.
  44. Yeom DW, Song YS, Kim SR, Lee SG, Kang MH, Lee S, *et al.* Development and optimization of a self-microemulsifying drug delivery system for atorvastatin calcium by using D-optimal mixture design. *Int J Nanomed* 2015;10:3865-77.
  45. Kamboj S, Rana V. Quality-by-design based development of a self-microemulsifying drug delivery system to reduce the effect of food on nelfinavir mesylate. *Int J Pharm* 2016;501:311-25.
  46. Constantinides PP, Scalart JP. Formulation and physical characterization of water-in-oil microemulsions containing long-versus medium-chain glycerides. *Int J Pharm* 1997;158:57-68.
  47. Ansari KA, Pagar KP, Anwar S, Vavia PR. Design and optimization of self-microemulsifying drug delivery system (SMEDDS) of felodipine for chronotherapeutic application. *Braz J Pharm Sci* 2014;50:203-12.
  48. Madan JR, Sudarshan B, Kadam VS, Kamal D. Formulation and development of self-microemulsifying drug delivery system of pioglitazone. *Asian J Pharm* 2014;8:296-233.
  49. Danaei M, Dehghankhold M, Ataei S, Davarani FH, Javanmard R, Dokhani A, *et al.* Impact of particle size and polydispersity index on the clinical applications of lipidic nanocarrier systems. *Pharmaceutics* 2018;10:1-17.
  50. Barhoum A, García-Betancourt ML, Rahier H, Van Assche G. Physicochemical characterization of nanomaterials: Polymorph, composition, wettability, and thermal stability. In: Barhoum A, Makhoulf AS, editors. *Emerging Applications of Nanoparticles and Architecture Nanostructures Current Prospects and Future Trends*. Amsterdam, Netherlands: Elsevier; 2018. p. 255-78.
  51. Joseph E, Singhvi G. Multifunctional nanocrystals for cancer therapy: A potential nanocarrier. In: Grumezescu AM, editor. *Nanomaterials for Drug Delivery and Therapy*. Amsterdam, Netherlands: Elsevier; 2019. p. 91-116.
  52. Losso JN, Khachatryan A, Ogawa M, Godber JS, Shih F. Random centroid optimization of phosphatidylglycerol stabilized lutein-enriched oil-in-water emulsions at acidic pH. *Food Chem* 2005;92:737-744.
  53. Roland I, Piel G, Delattre L, Evrard B. Systematic characterization of oil-in-water emulsions for formulation design. *Int J Pharm* 2003;263:85-94.
  54. de Sousa IP, Steiner C, Schmutzler M, Wilcox MD, Veldhuis GJ, Pearson JP, *et al.* Mucus permeating carriers: Formulation and characterization of highly densely charged nanoparticles. *Eur J Pharm Biopharm* 2015;97:273-279.
  55. Mundada VP, Sawant KK. Enhanced oral bioavailability and anticoagulant activity of dabigatran etexilate by self-micro emulsifying drug delivery system: Systematic development, *in vitro*, *ex vivo* and *in vivo* evaluation. *J Nanomed Nanotechnol* 2018;9:480-92.
  56. Qi X, Wang L, Zhu J, Hu Z, Zhang J. Self-double-emulsifying drug delivery system (SDEDDS): A new way for oral delivery of drugs with high solubility and low permeability. *Int J Pharm* 2011;409:245-251.
  57. Cui J, Yu B, Zhao Y, Zhu W, Li H, Lou H, *et al.* Enhancement of oral absorption of curcumin by self-microemulsifying drug delivery systems. *Int J Pharm* 2009;371:148-55.
  58. Patel MJ, Patel NM, Patel RB, Patel RP. Formulation and evaluation of self-microemulsifying drug delivery system of lovastatin. *Asian J Pharm Sci* 2010;5:266-75.
  59. Bachhav YG, Patravale VB. SMEDDS of glyburide: Formulation, *in vitro* evaluation, and stability studies. *AAPS PharmSciTech* 2009;10:482-7.

## APPENDIX

In this research, a simple UV-visible spectrophotometric method was developed for determination of the amount of AST in SMEDS formulations. A standard calibration curve for AST absorbance and concentration was firstly prepared. An organic solvent mixture of dichloromethane (DCM) and methanol (MeOH) in 1:4 v/v ratio was used to dissolve AST into solution at various concentrations, and the wavelength corresponding to maximum absorbance of AST was specifically found at 480 nm. Measurement of AST concentrations obeyed the Beer-Lambert law within the range of 0.5–5  $\mu\text{g}/\text{ml}$ . A linear equation obtained by the least square regression method was  $y = 0.2163x + 0.0004$  with a coefficient of determination ( $R^2$ ) of 0.99999 as shown in Figure a1. We then carried out analyses of samples prepared with all excipients presented in the SMEDS (castor oil: Cremophor<sup>®</sup> RH 40: Tween<sup>®</sup> 80 = 1:4:1) with and without AST to verify the absence of interference from the SMEDS ingredients on quantification of AST. The blank SMEDS without AST showed no peak at the wavelength of 480 nm and thus no potential interference from the SMEDS compositions [shown as the red line in Figure a2] while the AST-loaded SMEDS displayed an absorption spectrum at the same wavelength (exhibited as the black line). Furthermore, as we studied *in vitro* release of AST from various dosage forms in three sequentially changing dissolution media, standard curves of AST at different pH were also provided in Figure a3.

The AST quantification method in our research was validated for several parameters including linearity, accuracy, and precision as per the International Council for Harmonisation guideline. The values of the relative SD and the percent recovery were found to be satisfactory indicating that the method was sufficiently precise and accurate and hence could be used for a routine analysis of AST in SMEDS formulations. For sensitivity of the method, AST SMEDS at a 5-time lower concentration than that of in our formulations could still yield a detectable absorbance value at  $\lambda = 480$  nm. However, we are also currently working on development and validation of the analytical method for AST in SMEDS formulations using high performance liquid chromatography with a UV-visible detector to assay AST content in SMEDS in our recent continual project.

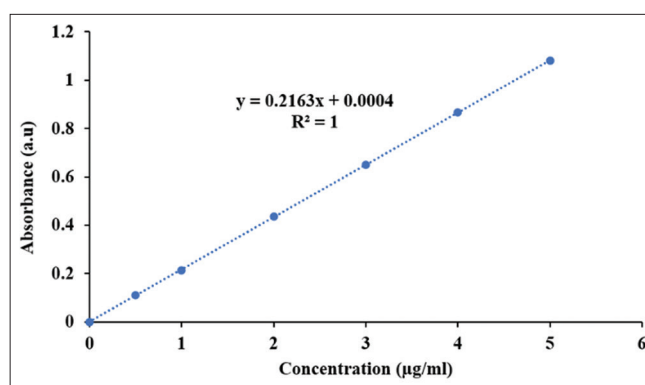


**Figure A1:** A standard calibration curve of astaxanthin in dichloromethane: methanol (1:4 v/v) at  $\lambda=480$  nm

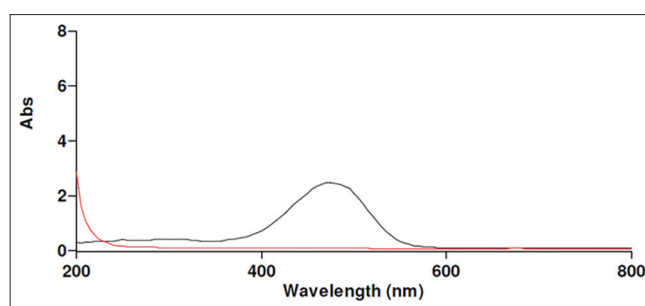


**Figure A2:** Absorption spectra of the blank self-microemulsifying delivery system (SMEDS) (red) and astaxanthin SMEDS (black) showing a maximum absorbance at  $\lambda=480$  nm

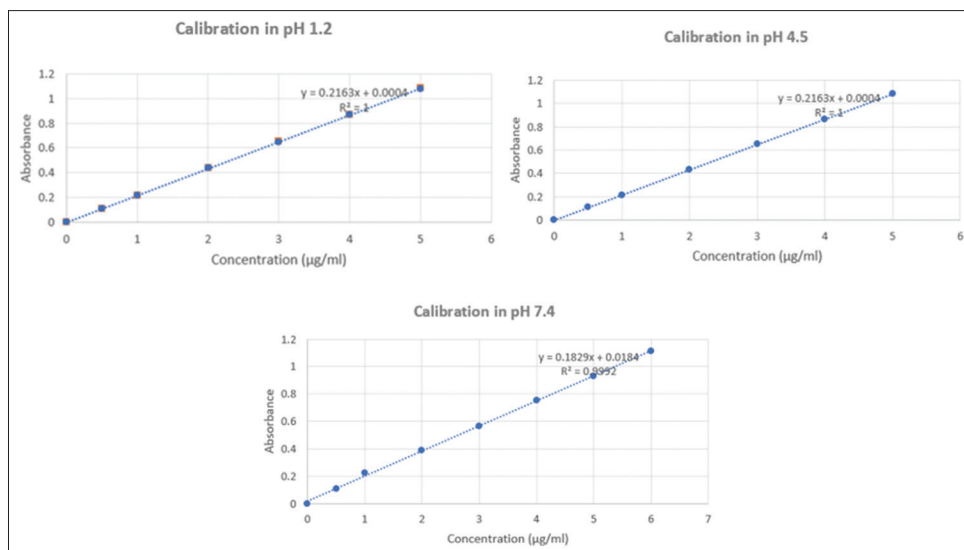


**Figure A3:** Standard calibration curves of astaxanthin at three different pH: pH 1.2, pH 4.5, and pH 7.4 at  $\lambda=480$  nm